Amoroso, S.M., Compagnoni, C.M., Ghetti, A., Gerrer, L., Spinelli, A.S., Lacaita, A.L., and Asenov, A. (2013) Investigation of the RTN Distribution of nanoscale MOS devices from subthreshold to on-state. IEEE Electron Device Letters, 34 (5). pp. 683-685. ISSN 0741-3106

Investigation of the RTN Distribution of Nanoscale MOS Devices From Subthreshold to On-State

Salvatore M. Amoroso, *Member, IEEE*, Christian Monzio Compagnoni, *Member, IEEE*,
Andrea Ghetti, *Member, IEEE*, Louis Gerrer, Alessandro S. Spinelli, *Senior Member, IEEE*,
Andrea L. Lacaita, *Fellow, IEEE*, and Asen Asenov, *Fellow, IEEE*

***Abstract*— This letter presents a numerical investigation of the statistical distribution of the random telegraph noise (RTN) amplitude in nanoscale MOS devices, focusing on the change of its main features when moving from the subthreshold to the on-state conduction regime. Results show that while the distribution can be well approximated by an exponential behavior in subthreshold, large deviations from this behavior appear when moving toward the on-state regime, despite a low probability exponential tail at high RTN amplitudes being preserved. The average value of the distribution is shown to keep an inverse proportionality to channel area, while the slope of the high-amplitude exponential tail changes its dependence on device width, length, and doping when moving from subthreshold to on-state.**

***Index Terms*— Flash memories, MOSFETs, random telegraph noise, semiconductor-device modeling.**

I. INTRODUCTION

RANDOM telegraph noise (RTN) represents one of the most important reliability issues for modern deca-nanometer MOS technologies, attracting many research efforts devoted to the understanding of its statistical features [1]–[5]. In particular, the statistical distribution of the RTN amplitude has been widely investigated [4], [6], [7], due to its importance in determining the RTN impact on the operation of digital devices, such as Flash memories and SRAM cells [8], [9]. So far, results have shown an exponential behavior for this statistical distribution [2], [4], coming from a dominant contribution of percolative channel conduction on the threshold-voltage shift (ΔV_T) obtained after electron capture/emission in the RTN trap [4], [10]. However, these results have been obtained extracting ΔV_T at low currents (subthreshold or near threshold regime), and only few attempts have been made to investigate the ΔV_T distribution in the on-state [11]. Moreover, the validity of the exponential behavior in deeply-scaled devices with channel dimensions of just a few tens of nanometer has never been verified.

In this letter, we show that the statistical distribution of the RTN amplitude deviates from a pure exponential when moving from the subthreshold to the on-state regime and when severely scaling device dimensions, preserving, however, an exponential tail at high ΔV_T. Results reveal that while the average value of the distribution ($\langle \Delta V_T \rangle$) keeps an inverse proportionality to channel area both in subthreshold and in on-state conditions, the slope of the high-ΔV_T tail moves from an inverse proportionality to the square root of device width (W) and length (L) in subthreshold to an inverse proportionality to W and L in the on-state regime, also reducing its dependence on substrate doping. This is interpreted in terms of a more uniform conduction when moving from subthreshold to on-state, with a lower impact of atomistic doping on ΔV_T.

II. SIMULATION METHODOLOGY

We performed 3-D numerical simulations of a Flash cell with a $t_{\text{ox}} = 8$ nm tunnel oxide, a 70-nm polysilicon floating gate, and a 4/3/5 nm oxide-nitride-oxide interpoly dielectric. Source and drain doping have a peak concentration of 10^{20} cm^{-3} at the silicon surface and a Gaussian vertical profile with a junction depth of 25 nm. Substrate is uniformly doped with a boron concentration equal to $N_A = 5 \times 10^{17}$, 2×10^{18} or 4×10^{18} cm^{-3}. Three possible values of cell W and L were assumed, namely, 32, 64, and 128 nm, leading to nine cell geometries. Further details on the device can be found in [12], where the cell is referred to as “rounded edges.”

The statistical distribution of the RTN amplitude was calculated by means of a Monte Carlo procedure [12], where a large number of cells having a different atomistic configuration of substrate doping and a different position of a single RTN trap over the channel area were simulated. From each simulation, ΔV_T was obtained as the change of the floating-gate potential allowing the same current to flow in the cell for the empty (neutral) and the filled (negatively charged) RTN trap. A read current of 100 nA $\times$ W/L, 2 μA $\times$ W/L, and 8 μA $\times$ W/L was assumed for ΔV_T evaluation in the subthreshold, near threshold and on-state regime, respectively, as shown in Fig. 1, where the drain current versus gate voltage ($I_D - V_{\text{FG}}$) curves are shown for many atomistically different devices in the case of $W = L = 32$ nm and $N_A = 2 \times 10^{18}$ cm^{-3}. Simulations were carried out by means of the drift-diffusion module of the gold standard simulations (GSS) atomistic simulator GARAND [13], activating density-

---

Manuscript received January 7, 2013; accepted February 26, 2013. Date of publication April 1, 2013; date of current version April 22, 2013. This work was supported by the European Commission via the MORDRED Project 261868. The review of this letter was arranged by Editor M. Östling.

S. M. Amoroso and L. Gerrer are with the University of Glasgow, Glasgow G12 8QQ, U.K. (e-mail: salvatore.amoroso@glasgow.ac.uk).

C. Monzio Compagnoni, A. S. Spinelli, and A. L. Lacaita are with the Dipartimento di Elettronica, Informazione e Bioingegneria, Politecnico di Milano, Milano 20133, Italy.

A. Ghetti is with the R&D Technology Development, Micron Technology Inc., Agrate Brianza 20041, Italy.

A. Asenov is with the University of Glasgow, Glasgow G12 8QQ, U.K., and also with Gold Standard Simulation Ltd., Glasgow G12 8LT, U.K.

Color versions of one or more of the figures in this letter are available online at http://ieeexplore.ieee.org.

Digital Object Identifier 10.1109/LED.2013.2250477

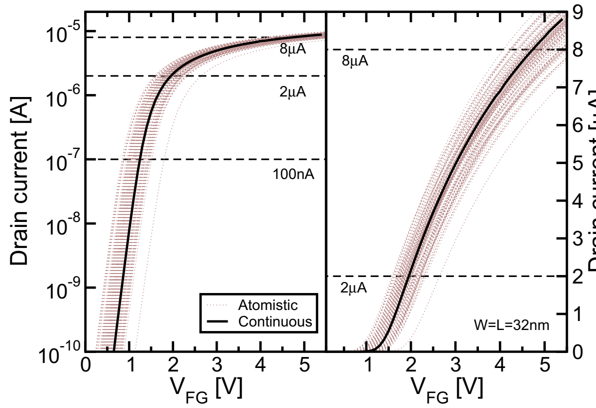

Fig. 1. Simulated I_D-V_{FG} curve for many atomistically different devices with $W = L = 32$ nm and $N_A = 2 \times 10^{18}$ cm^{-3}. Dashed lines highlight the I_D values used for ΔV_T definition in the subthreshold, near threshold, and on-state regime. The curve corresponding to a continuous substrate doping is also shown.

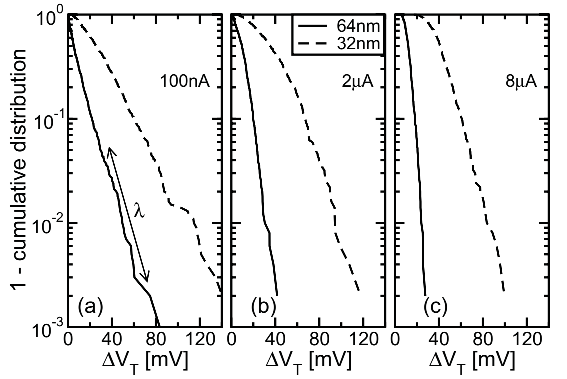

Fig. 2. Simulated ΔV_T distribution in the case of $W = L = 64$ nm and $W = L = 32$ nm ($N_A = 2 \times 10^{18}$ cm^{-3}) at (a) $I_D = 100$ nA, (b) 2 μA, and (c) 8 μA.

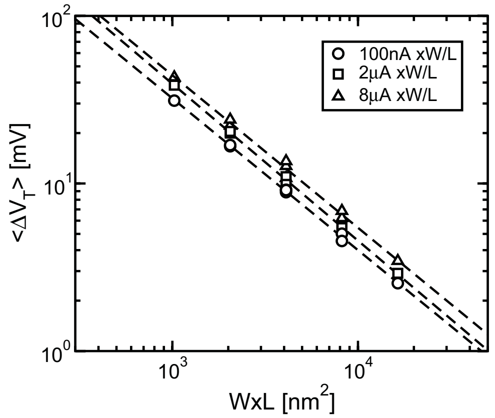

Fig. 3. Simulated $\langle \Delta V_T \rangle$ as a function of channel area $W \times L$ at $I_D = 100$ nA, 2 μA, and 8 μA in the case of $N_A = 2 \times 10^{18}$ cm^{-3}.

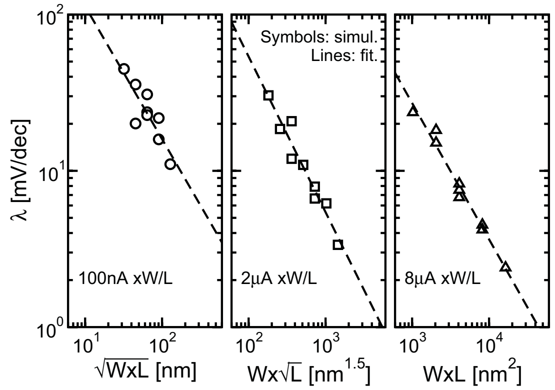

(a) (b) (c)

Fig. 4. Simulated λ at (a) $I_D = 100$ nA, (b) 2 μA, and (c) 8 μA as a function of different functions of W and L, for $N_A = 2 \times 10^{18}$ cm^{-3}.

gradient quantum corrections to correctly reproduce the electrostatic effect of dopants and quantum confinement in the channel. Note that, when referring to the on-state regime, these simulations underestimate the effect of localized point charges on device current, due to the lack of a correct implementation of the impact of these charges on carrier transport [14], [15]. As a consequence, these simulations underestimate variability in the drain current coming from atomistic doping [15] and the reduction of this current following the filling of RTN traps [16] in the on-state. This means that the on-state ΔV_T here reported are representative only of the electrostatic effect of RTN traps, with the additional contribution given by mobility modulation around the traps neglected.

III. SIMULATION RESULTS

Fig. 2(a) shows the simulated ΔV_T distributions at $I_D = 100$ nA in the case of $W = L = 64$ nm and $W = L = 32$ nm, with $N_A = 2 \times 10^{18}$ cm^{-3}. Both of the distributions can be reasonably approximated with an exponential trend, in agreement with what reported in [2] and [4], with a slope λ (units: [mV/dec]) increasing with device scaling. Fig. 2(b) and (c) reveal, instead, that the distributions significantly deviate from a pure exponential behavior when increasing the read current to 2 μA (b) and 8 μA (c). In particular, moving to the on-state regime makes the distributions broader at high probabilities with respect to subthreshold case, but narrower at low probabilities, which are of more interest for technology reliability. This narrowing is the result of steeper distribution tails in the graph, which, however, can still be approximated with an exponential behavior with slope λ.

In order to understand these results in more detail, Fig. 3 shows that the simulated $\langle \Delta V_T \rangle$ increases as cell dimensions are scaled keeping an inverse proportionality to the channel area $W \times L$, with small reductions when moving from the on-state to the subthreshold regime [17], [18]. Fig. 4 shows, instead, that the slope of the high-ΔV_T tail of the distributions of Fig. 2 displays a different dependence on W and L in the (a) subthreshold, (b) near-threshold, and (c) on-state regimes; while λ is inversely proportional to $\sqrt{W \times L}$ in the first case [2], an inverse proportionality to $W \times \sqrt{L}$ appears in the second case [4] and to $W \times L$ in the third [7]. This change comes with a reduction of the absolute values of λ and reflects a reduction of the impact of atomistic doping and percolative channel conduction on ΔV_T when moving from the subthreshold to the on-state regime [19]. From the different dependences of $\langle \Delta V_T \rangle$ and λ on W and L appearing from Figs. 3 and 4(a), we expect deviations from the exponential behavior even in subthreshold as cell scaling proceeds.

Fig. 5 shows that the $\langle \Delta V_T \rangle$ and λ scaling trends are also affected by a different dependence on N_A; while the

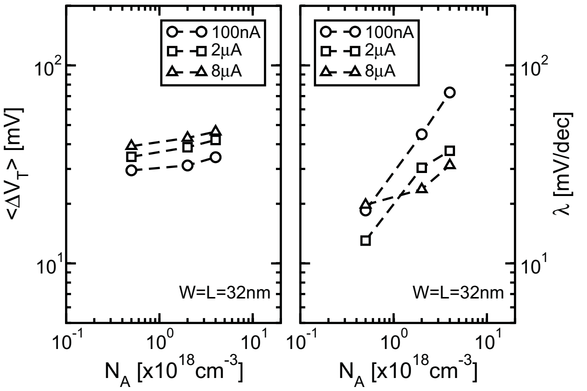

(a) (b)

Fig. 5. Simulated (a) $\langle \Delta V_T \rangle$ and (b) λ at $I_D = 100$ nA, 2 μA, and 8 μA as a function of N_A, for $W = L = 32$ nm.

former parameter has only a weak increase when increasing N_A, the latter displays a much stronger growth, being nearly proportional to $N_A^{0.65}$ at 100 nA [2], to $N_A^{0.5}$ at 2 μA [4], and to $N_A^{0.2}$ at 8 μA. This lower dependence of λ on N_A when increasing the read current represents a further proof of the lower impact of atomistic doping and percolative conduction on ΔV_T when moving from subthreshold to on-state.

IV. CONCLUSION

A detailed numerical investigation of the statistical distribution of the RTN amplitude of nanoscale MOS devices from the subthreshold to the on-state regime was presented. Results showed that the ΔV_T distribution has significant deviations from the purely exponential trend moving to the on-state, with device scaling giving the possibility of nonexponential behaviors even in subthreshold. The drain current dependence of the ΔV_T distribution was interpreted in terms of a lower impact of channel percolation and atomistic doping on ΔV_T when moving toward the on-state, as highlighted also by a weaker dependence of λ on N_A. The stronger λ dependence on W and L in on-state than in subthreshold should be considered in all those devices exploiting the strong inversion condition, such as SRAM and NOR Flash memories.

ACKNOWLEDGMENT

The authors would like to thank S. Markov, F. Adamu-Lema, and G. Roy from the University of Glasgow, Glasgow, U.K., for helpful discussions, and A. Benvenuti, A. Mauri, and A. Marmiroli from Micron Technology Inc., Agrate Brianza, Italy, for their support.

REFERENCES

[1] H. Kurata, K. Otsuga, A. Kotabe, S. Kajiyama, T. Osabe, Y. Sasago, S. Narumi, K. Tokami, S. Kamohara, and O. Tsuchiya, “The impact of random telegraph signals on the scaling of multilevel Flash memories,” in *Symp. VLSI Circuits Dig. Tech. Papers*, 2006, pp. 140–141.

[2] K. Fukuda, Y. Shimizu, K. Amemiya, M. Kamoshida, and C. Hu, “Random telegraph noise in Flash memories-model and technology scaling,” in *Proc. IEEE Int. Electron Devices Meeting*, Dec. 2007, pp. 169–172.

[3] C. Monzio Compagnoni, R. Gusmeroli, A. S. Spinelli, A. L. Lacaita, M. Bonanomi, and A. Visconti, “Statistical model for random telegraph noise in Flash memories,” *IEEE Trans. Electron Devices*, vol. 55, no. 1, pp. 388–395, Jan. 2008.

[4] A. Ghetti, C. Monzio Compagnoni, A. S. Spinelli, and A. Visconti, “Comprehensive analysis of random telegraph noise instability and its scaling in deca-nanometer Flash memories,” *IEEE Trans. Electron Devices*, vol. 56, no. 8, pp. 1746–1752, Aug. 2009.

[5] T. Nagumo, K. Takeuchi, T. Hase, and Y. Hayashi, “Statistical characterization of trap position, energy, amplitude and time constants by RTN measurement of multiple individual traps,” in *Proc. IEEE Int. Electron Devices Meeting*, Dec. 2010, pp. 628–631.

[6] A. Asenov, R. Balasubramaniam, A. R. Brown, and J. H. Davies, “RTS amplitudes in decananometer MOSFETs: 3-D simulation study,” *IEEE Trans. Electron Devices*, vol. 50, no. 3, pp. 839–845, Mar. 2003.

[7] K. Takeuchi, T. Nagumo, S. Yokogawa, K. Imai, and Y. Hayashi, “Single-charge-based modeling of transistor characteristics fluctuations based on statistical measurement of RTN amplitude,” in *Proc. Symp. VLSI Technol.*, Jun. 2009, pp. 54–55.

[8] C. Monzio Compagnoni, M. Ghidotti, A. L. Lacaita, A. S. Spinelli, and A. Visconti, “Random telegraph noise effect on the programmed threshold-voltage distribution of Flash memories,” *IEEE Electron Device Lett.*, vol. 30, no. 9, pp. 984–986, Sep. 2009.

[9] K. Takeuchi, T. Nagumo, and T. Hase, “Comprehensive SRAM design methodology for RTN reliability,” in *Proc. Symp. VLSI Technol.*, Jun. 2011, pp. 130–131.

[10] L. K. J. Vandamme, D. Sodini, and Z. Gingl, “On the anomalous behavior of the relative amplitude of RTS noise,” *Solid-State Electron.*, vol. 42, no. 6, pp. 901–905, Jun. 1998.

[11] B. Kaczer, J. Franco, M. Toledano-Luque, P. J. Roussel, M. F. Bukhori, A. Asenov, B. Schwarz, M. Bina, T. Grasser, and G. Groeseneken, “The relevance of deeply-scaled FET threshold voltage shifts for operation lifetimes,” in *Proc. IEEE Int. Rel. Phys. Symp.*, Apr. 2012, pp. 5A.2.1–5A.2.6.

[12] S. M. Amoroso, A. Ghetti, A. R. Brown, A. Mauri, C. Monzio Compagnoni, and A. Asenov, “Impact of cell shape on random telegraph noise in decananometer Flash memories,” *IEEE Trans. Electron Devices*, vol. 59, no. 10, pp. 2774–2779, Oct. 2012.

[13] [Online]. Available: http://www.goldstandardsimulations.com.

[14] C. Alexander, A. R. Brown, J. R. Watling, and A. Asenov, “Impact of scattering in ‘atomistic’ device simulations,” *Solid-State Electron.*, vol. 49, no. 5, pp. 733–739, May 2005.

[15] U. Kovac, C. Alexander, G. Roy, C. Riddet, B. Cheng, and A. Asenov, “Hierarchical simulation of statistical variability: From 3-D MC with ‘ab initio’ ionized impurity scattering to statistical compact models,” *IEEE Trans. Electron Devices*, vol. 57, no. 10, pp. 2418–2426, Oct. 2010.

[16] C. L. Alexander, A. R. Brown, J. R. Watling, and A. Asenov, “Impact of single charge trapping nano-MOSFETs-electrostatics versus transport effects,” *IEEE Trans. Nanotechnol.*, vol. 4, no. 3, pp. 339–344, May 2005.

[17] G. Fiori, G. Iannaccone, G. Molas, and B. De Salvo, “Dependence of the programming window of silicon-on-insulator nanocrystal memories on channel width,” *Appl. Phys. Lett.*, vol. 86, no. 11, pp. 113502-1–113502-3, Mar. 2005.

[18] R. Gusmeroli, A. S. Spinelli, C. Monzio Compagnoni, and D. Ielmini, “Threshold-voltage statistics and conduction regimes in nanocrystal memories,” *IEEE Electron Device Lett.*, vol. 27, no. 5, pp. 409–411, May 2006.

[19] H. Miki, N. Tega, M. Yamaoka, D. J. Frank, A. Bansal, M. Kobayashi, K. Cheng, C. P. D’Emic, Z. Ren, S. Wu, J.-B. Yau, Y. Zhu, M. A. Guillorn, D.-G. Park, W. Haensch, E. Leobandung, and K. Torii, “Statistical measurement of random telegraph noise and its impact in scaled-down high-k/metal-gate MOSFETs,” in *Proc. Int. Electron Devices Meeting*, 2012, pp. 450–453.